JOURNAL OF MATERIALS SCIENCE **34** (1999) 5075 – 5080

Highly oriented (Pb, La)TiO_3 thin films prepared by sol-gel process

JUNMO KOO, JAE HYEOK JANG, BYEONG-SOO BAE
Department of Materials Science and Engineering, Korea Advanced Institute of Science and Technology (KAIST), Taejon 305-701, Korea
E-mail: bsbae@sorak.kaist.ac.kr

Highly oriented lead lanthanum titanate (PLT) thin films on MgO (100) and *c*-plane sapphire single-crystal substrates have been prepared using the sol-gel process. The orientation and the mechanism of the highly preferred oriented PLT films derived sol-gel process have been investigated. The sol-gel PLT films fabricated on MgO (100) and *c*-plane sapphire substrates grow preferentially with (100) and (111) crystallographic orientations respectively, regardless of the film thickness and La content. In addition, it is confirmed that the tetragonality of the PLT perovskite structure decreases with an increase of La content. The *a*-axis orientation of the sol-gel PLT film on MgO (100) substrate is controlled only by formation of the intrinsic tensile stress during the crystallization of the film. © *1999 Kluwer Academic Publishers*

1. Introduction

Ferroelectric thin films of the lanthanum-modified lead zirconate titanate (PLZT) system have attracted great interest for various applications such as high dielectric, pyroelectric, piezoelectric, and electro-optic devices [1–6]. Among these applications, it is very important for electro-optic devices applications to prepare high-quality epitaxial thin films to take advantage of the anisotropic properties of these ferroelectric materials.

Early work on fabrication of PLZT thin films were based mainly on vacuum deposition techniques such as sputtering and evaporation [2, 3, 5]. Many researchers have succeeded in growing of PLZT thin films epitaxially on $SrTiO_3$, MgO, and sapphire substrates using the rf magnetron sputtering and the pulsed laser deposition [1–7]. Although vacuum deposition techniques are good methods for the epitaxial growth of the PLZT thin films, they have a serious problem that occurs due to the processing complexity of multicomponent systems. Recently, sol-gel processing of PLZT thin films has been reported due to such advantages as precise composition control and homogeneity, low temperature synthesis, large-area deposition, low cost, and a short fabrication process [8–10]. However, the epitaxial growth mechanism of the sol-gel film is more difficult than that of such vacuum deposited films as rf sputtered and chemical vapor deposited films. The latter are grown *in situ* with the following mechanisms: condensation of vaper atoms and ions on the substrate surface, nucleation, and growth. The nucleation initiated on the surface of the substrate having a lattice match with the film leads to the epitaxial growth. However, in the case of the sol-gel process, the epitaxial growth is related to the crystallization of the solid amorphous film prepared by coating and drying. The general nuclei form not only within the bulk but also at the interface between the film and the substrate for the sol-gel process. The heterogeneous nucleation at the interface between the film and the lattice-matched substrate would lead to the formation of highly preferred orientation or epitaxial thin films. The sol-gel process is very difficult to control the nucleation rate and the location of the nuclei during the crystallization of amorphous film. Thus, the detailed growth mechanism of the sol-gel process has not been investigated sufficiently.

In this paper, we have prepared highly oriented PLT thin films on MgO (100) and *c*-plane sapphire single-crystal substrates using the sol-gel process. Growth has been studied as a function of La concentration and the film thickness. The growth mechanism of the sol-gel process derived PLT thin films was investigated using the X-ray diffraction (XRD) analyses. Instead of the PLZT system, the reason for the selection of composition without zirconium content, PLT system, is that this system has been known to be better for the future optical applications due to its finer grain size and higher transparency than the PLZT system [3, 11].

2. Experimental

PLT films were prepared with the general chemical formula $Pb_{1-x}La_xTi_{1-x/400}O_3$ (it is called PLTx), where $x = 5$, 10, 15, 20, 28 mol %. A precise procedure for preparing the precursor solution is shown in Fig. 1. Lead acetate ($Pb(CH_3COO)_2 \cdot 3H_2O$, 99.999%, Aldrich Chemical Co.), lanthanum nitrate ($La(NO_3)_3 \cdot 6H_2O$, 99.99%, Aldrich Chemical Co.), and titanium isopropoxide ($Ti[(CH_3)_2CHO]_4$, 99.999%, Aldrich Chemical Co.) were used as precursors. The sol-gel PLT thin films containing large La contents have rarely been

TABLE I Characteristics of PLT films and substrates

Properties	PLT5 ∼ PLT28	MgO[a]	Sapphire[a]
Crystal system	Tetragonal	Cubic	Hexagonal
Crystal structure	Perovskite	NaCl	Corundum
	$a = 0.397 \sim 0.402$		$a = 0.476$
Lattice parameter (nm)		0.420	
	$c = 0.416 \sim 0.412$		$c = 1.299$
Thermal expansion			par. c: 8.3×10^{-6}
coefficient (/°C)	$\sim 1 \times 10^{-6}$ [b]	13.63×10^{-6}	perp. c: 7.5×10^{-6}
Refractive index			
(at 633 nm)	∼2.5[c]	1.74	1.77

[a]These products and the data are provided form Target Materials, Inc., U.S.A. [b,c]Based on the reference [10].

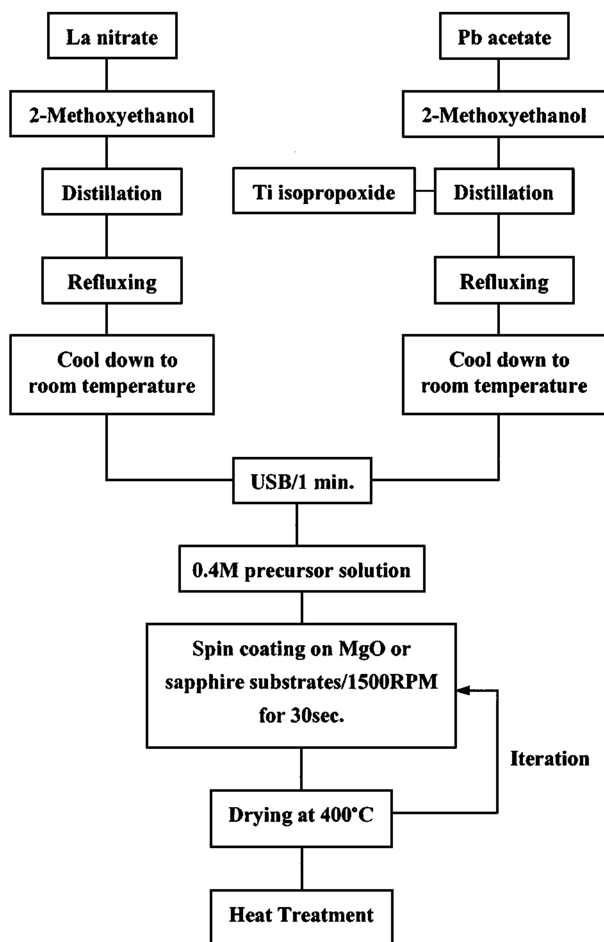

Figure 1 Flow chart for preparation of PLT solution and thin films.

fabricated due to the low solubility of La precursors in alcohol. However, the sol-gel PLT15∼PLT28 thin films were fabricated successfully using lanthanum nitrate as La precursor recently [12]. Also, 5 mol % excess Pb was incorporated since it was found that excess PbO aids significantly in compensating PbO loss when the normal stoichiometric compositions were used. Methoxyethanol ($CH_3OCH_2CH_2OH$, 99.9%, Aldrich Chemical Co.) was used as a solvent to facilitate the dehydration by heating because it boils at 125 °C. Lead acetate was dissolved in methoxyethanol on heating at 120 °C for 6 h to decrease residual water and titanium isopropoxide was then added. The solution was again heated for 6 h to be re-distilled and refluxed at 80 °C for 10 h. The precursor mixture solution was then cooled to room temperature. The lanthanum solution was made by a similar process.

The selection of the substrate is very important for the highly preferred oriented thin film because the degree of matching between the film and the substrate at the lattice parameter and the crystal structure strongly affects. The temperature dependence of lattice parameters, i.e., thermal expansion coefficients, is also an important parameter since ferroelectric materials usually have structural phase transitions during cooling from deposition temperature. In addition, the refractive index of the substrate must be lower than that of the film for optical waveguide application. From the viewpoint of the crystallographic properties, MgO (100) and *c*-plane sapphire single crystals are used as suitable substrates in this study. Various properties such as the crystal structure, the thermal expansion coefficient, the refractive index of PLT5∼PLT28 films, MgO, and sapphire substrates are summarized in Table I. It is known that the oxygen ion configuration of (100) plane of MgO substrate with (100) plane of cubic perovskite phase exhibits good lattice matching. The *c*-plane of sapphire substrate and the (111) plane of cubic perovskite phase also have similar lattice matching [13, 14]. Prior to coating, the substrates (25 mm × 25 mm × 0.5 mm) were thoroughly cleaned. A standard semiconductor cleaning procedure was used to clean all substrates. Inorganic contaminants were removed in a solution of $H_2O:NH_4OH:H_2O_2$ and $H_2O:HCl:H_2O_2$ in the volume ratio of 10 : 1 : 1, respectively. Organic contaminants were removed in boiling trichloroethylene for 5 min. The substrates were then rinsed in acetone, ethanol, and distilled water, and dried with nitrogen.

Solutions were spin-coated on these substrates using a spin coater (EC101-R485, Headway Research Inc.) at 1500 rpm for 30 s. The green films were then dried at 400 °C on a hot plate for 10 min to evaporate nitrates as well as the residual organic solvent. A coating yields about 50 nm thickness. This procedure was repeated until the desired thickness was obtained. The films were heat-treated with 5 °C/min to 700 °C holding for 30 min to be crystallized. When the heating temperature is high, the heterogeneous nucleation and growth of perovskite grain at the interface between the film and the substrate occur easily because of high thermal energy. Heterogeneous nucleation at the interface between

the film and the lattice-matched substrate would lead to the formation of highly preferred oriented and/or epitaxial thin films. However, when the temperature is too high (>800 °C), microcracks are found in the film due to thermal shock and dramatic evaporation of Pb species. Therefore, the processing temperature used in this study was 150 °C higher than the crystallization temperature (≈550 °C) obtained from the differential thermal analysis (DTA) and the thermogravimetry analysis (TGA) [15]. And all the films were cooled at 2 °C/min in the atmosphere to prevent cracks caused by thermal shock during cooling.

The crystalline phase and orientation of the PLT film fabricated on MgO and sapphire substrates were examined using X-ray diffraction (D/MAX-RC, Rigaku Co.). Rocking curves were obtained to estimate the degree of film orientation. The microstructure and thickness of the films were observed using a scanning electron microscope (Philips 535M, Philips Inc.).

3. Results and discussion

3.1. Effect of film thickness

XRD patterns of the PLT5 composition films fabricated on MgO (100) single crystal substrates over a range of film thickness are shown in Fig. 2a. All the films show single perovskite phase without any other noticeable phase such as pyrochlore phase, and have main (100) and (200) peaks with small peaks of (110) and (111) planes. The PLT thin film is highly a-axis oriented, and the intensity of the main peaks increase with increasing film thickness. Also, the (110) and (111) peaks increase gradually with film thickness according to the data in Fig. 2a. The orientation of (100) plane is enhanced until the film thickness becomes the critical value (≈500 nm). Since the films thicker than the critical film thickness are too bulky to control the nucleation site, they provide heterogeneous nucleation sites of the other planes such as (110) and (111) planes as well as the nucleation of the main peak of (100) plane in the film. Heterogeneous nucleation at the interface between the layers would cause the formation of randomly oriented grains in the film. Thus, the orientation of (100) plane is not maintained over the critical film thickness. This would be confirmed in the SEM micrographs of PLT5 thin films on MgO substrates with various film thickness as shown in Fig. 3. The thicker film in Fig. 3a has many spherical grains in the whole cross section of the film, while the film in Fig. 3b exhibits a dence and clean cross-section. The grains at the interface between the film and the surface is grown to (100) plane for a-axis orientation, but the grains in the film is grown to the other planes such as (111) and (110) planes. This result suggests that the interface between the film and the surface is not the main heterogeneous nucleation sites for the film thicker than the critical value.

XRD patterns of the PLT films fabricated on c-plane sapphire single crystal substrates are shown in Fig. 2b. The PLT films are highly (111) oriented with small peaks in the XRD patterns. The variation in the XRD pattern as a function of film thickness is similar to that of the PLT films on the MgO substrates. For the low film thickness, the intensity of the main (111) peak increases with increasing the film thickness, but the (100), (200) and (110) peaks also increase gradually when the film thickness becomes over the critical value.

3.2. Effect of PLT composition

XRD patterns of the PLT films (≈350 nm thickness) having different La content fabricated on MgO (100) substrates are shown in Fig. 4. For the films on MgO substrates, main (100) and (001) peaks are observed

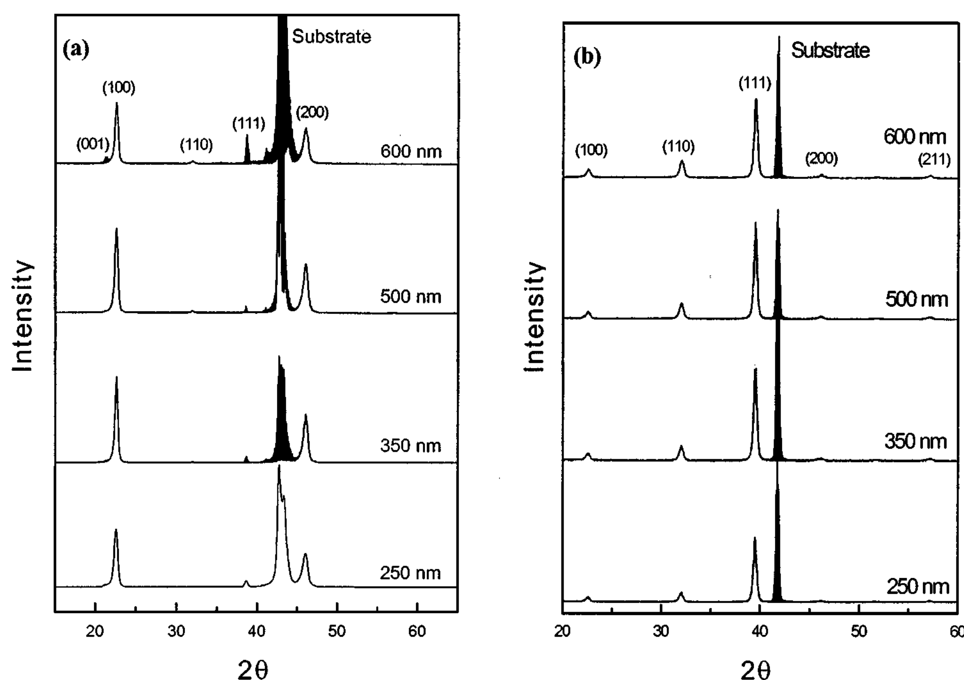

Figure 2 XRD patterns of PLT5 films on (a) MgO and (b) sapphire substrates as a function of the film thickness.

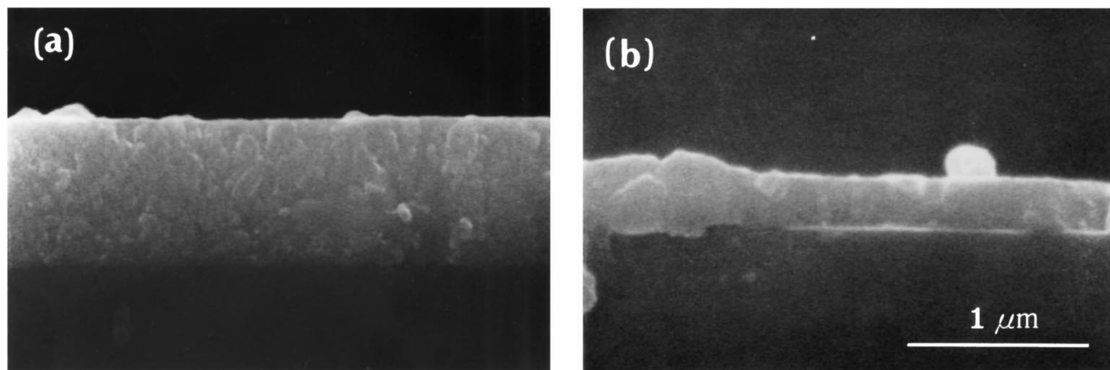

Figure 3 SEM micrographs of PLT5 thin films on MgO substrates with (a) 700 nm, and (b) 250 nm thicknesses.

for the low La content, but only (100) peak is detected when the La content is more than 20 mol %, as shown in Fig. 4a. As the La content in the film increases, the tetragonality of PLT perovskite structure decreases, which means the tetragonal structure of the PLT films changes to the cubic structure in the film [16]. Thus, the main (100) and (001) peaks are merged with increasing La content in the film.

The (111) peak is dominant regardless of the La content for the films on sapphire substrates as shown in Fig. 4b. The main (111) peak shifts to higher 2θ, approaching the (0001) peak of the sapphire substrate with increasing La content. It is also found that the intensity of main (111) peaks increase comparing with other peaks of (100) and (110) planes. This is due to better lattice match between the (111)-oriented PLT film and the c-plane sapphire substrate with increasing La content in the film by changing the tetragonal structure to the cubic structure in the PLT films.

The rocking curves as a function of La content for the PLT films on MgO and sapphire substrates are shown in Fig. 5. The full-widths-at-half-maximums (FWHM) values of the XRD rocking curves are about 4.2–4.5 and 0.15–0.3 for the films on MgO and sapphire substrates, respectively. The narrower rocking curves of the films on sapphire substrates compared with those of the films on the MgO substrates indicate that the PLT film on a sapphire substrate has better crystallographic alignment. This is due to better lattice match for the PLT films on sapphire substrates compared with that for the PLT films on the MgO substrates. This can be found when the oxygen-to-oxygen distances of the PLT28 film, the sapphire and MgO substrates are calculated, respectively. The calculated lattice mismatch, m ($m = |(a_f - a_s)/a_s|$, where a_f and a_s are the oxygen-to-oxygen distances of a film and a substrate, respectively) for the PLT28 film on MgO substrate, is 5.95%. On the other hand, the m value for the PLT28 film on sapphire substrate is 4.87%. Also, the much wider FWHM value of the rocking curves for the films on MgO substrates suggests that these films consist of a complete z-axis orientation and low angle grain boundaries in the x-y plane [17]. Thus, the relative large mismatch and the uncompleted orientation configuration of PLT film on MgO substrate caused the much wider FWHM values comparing with sapphire substrate.

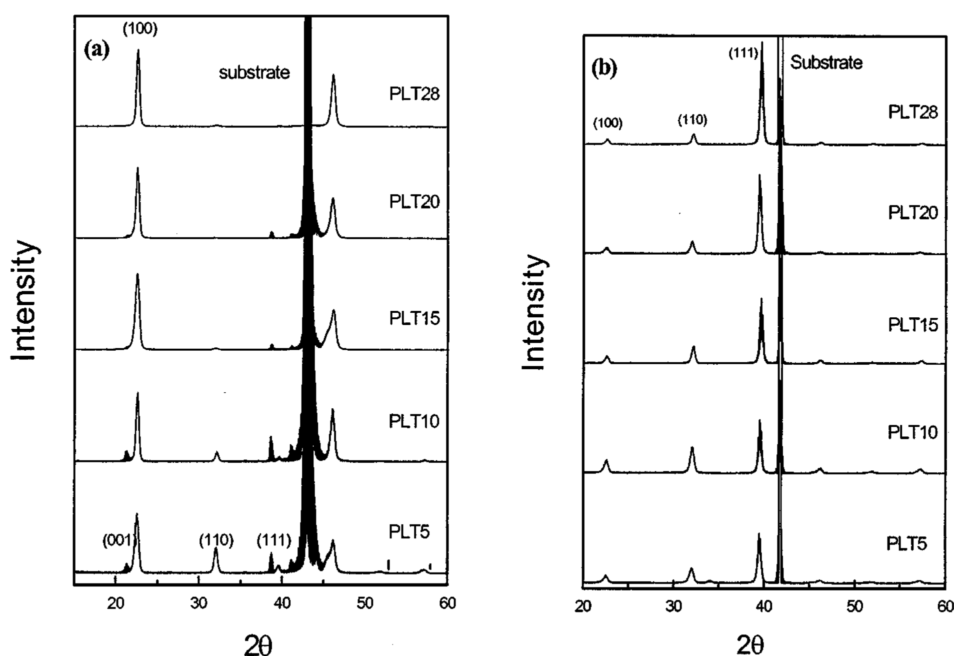

Figure 4 XRD patterns of PLT films on (a) MgO and (b) sapphire substrates as a function of the La content.

3.3. Epitaxial growth mechanism

Generally, the total stress which occurs in the deposited film is divided into four stresses while fabricating the film:

$$\sigma_{tot} = \sigma_{tr} + \sigma_{th} + \sigma_{ep} + \sigma_{in}$$

where σ_{tr} is the transformation stress by transformation from the cubic structure to the tetragonal structure at the Curie temperature, σ_{th} is the thermal stress by the difference of the thermal expansion coefficients between a film and a substrate, σ_{ep} is the misfit stress by difference of the lattice parameters between a film and a substrate, and σ_{in} is the intrinsic stress by the deposition condition [18–24]. Among these stresses, σ_{th} may be ignored since the compressive σ_{th} at the temperature range from the heating temperature to the Curie temperature is compensated with the tensile σ_{ep}. And σ_{th} at the temperature range from the Curie temperature to room temperature, which is too small to affect the film orientation [19]. σ_{tr} is also released during the cooling step by producing the domain-wall structure with 90° twins of *a*-axis and *c*-axis orientations [24]. Thus, it is thought that the orientation of the epitaxial ferroelectric films is mainly determined by the intrinsic stress in the film [21–23]. While the films deposited via sputtering create compressive stress in the films due to atomic peening in which high energy particles are reflected at the target and bombard the growing films [22]. Thus, the PLZT films by sputtering grow with *c*-axis orientation to remove the compressive residual stress. On the other hand, in the sol-gel process, a disordered solid amorphous film is made after coating and drying. The crystallization of the films, which changes from the disordered state to a more ordered state, is then accompanied by a decrease in volume and the formation of tensile stress in the films [22]. Therefore, the films are considered to grow with *a*-axis orientation to remove the tensile residual stress. The high temperature XRD patterns of the amorphous PLT5 films ($\approx$350 nm thickness) on MgO (100) substrates are investigated with changing in the temperature of the samples. The rate of heating and cooling was 5 and 2 °C/min respectively which were same with the heating schedule of the fabrication of PLT film. The PLT5 composition is chosen because the (100) and (001) planes can be distinguished as shown in Fig. 5a due to the tetragonality of PLT5 film is higher than the other compositions of the PLT films as illustrated in previous report [16]. The high temperature XRD patterns of the films as a function of the temperature are shown in Fig. 6. According to the thermal analysis, which was previously reported, the crystallization temperature of the PLT film is considered to be about 550 °C [15]. When the PLT5 film deposited by sol-gel process is heated to 600 °C, which is above the crystallization temperature, the film is crystallized with *a*-axis orientation to remove the tensile stress in the film created by the crystallization. When the film is heated to 700 °C to enhance the grain growth, a tensile stress is produced by the difference of the thermal expansion coefficients of the PLT film and a substrate. Cooling the film to 600 °C which is above the Curie temperature of the film (about 450 °C), can cause compressive stress, σ_{th} in the film as a result of the difference of the thermal expansion coefficients between the film and a substrate. However, the *a*-axis orientation of the film is not changed during the heating and cooling step of the film as shown in Fig. 6b ∼ c due to the previous relation between σ_{th} and σ_{ep}. Also, the orientation of the film is invariable even though the further cooling the film to 300 °C, which can create the transformation stress in the film. Thus, the thermal stress induced by thermal history except the intrinsic stress, σ_{in} does not affect the orientation of this film.

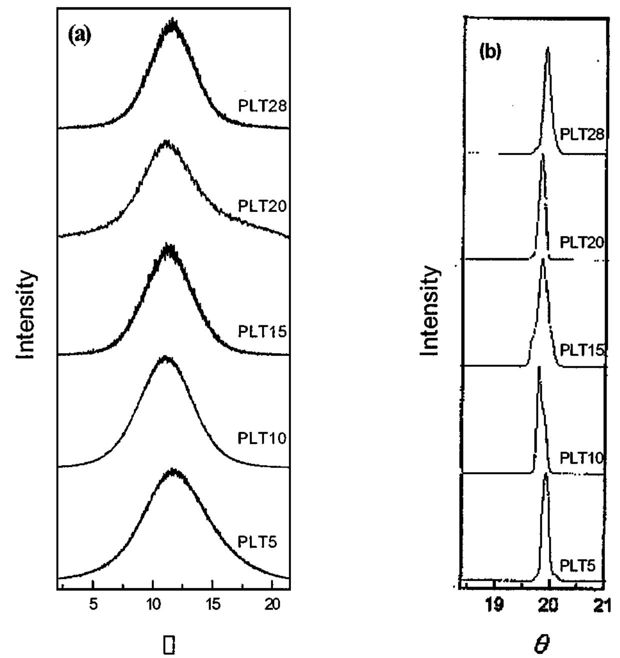

Figure 5 Rocking curves of PLT films for (a) (100) plane on MgO substrates and (b) (111) plane on sapphire substrates.

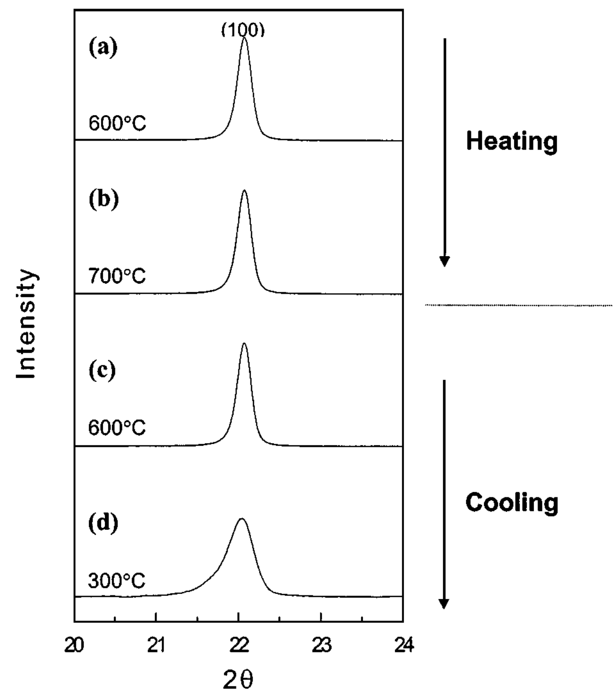

Figure 6 High temperature XRD patterns of PLT5 thin films on MgO(100) substrates during the heating and cooling step.

However, the (100) plane peak shows the shoulder including the (001) plane peak as shown in the Fig. 6d. The (100) plane peak shifts slightly to lower 2θ due to the transition from the cubic to the tetragonal structure passing the Curie temperature. The orientation of the sol-gel films is determined only by the formation of intrinsic tensile stress in the films during crystallization, regardless of an other terms of stress in the films. Therefore, the a-axis orientation of PLT films on a MgO (100) substrate occurs in the sol-gel process, while the c-axis orientation of PLT film is generally dominant in such vacuum deposition techniques as sputtering.

4. Conclusions

Highly oriented PLT thin films are prepared on MgO (100) substrates and c-plane sapphire substrates by a sol-gel process. The films are heat-treated at 700 °C, which is higher than the crystallization temperature to enhance the heterogeneous nucleation and growth of the PLT perovskite grains at the interface between the film and the substrate. Although the PLT films on MgO and sapphire substrates have (100) and (111) orientations, respectively, the epitaxy of the films is affected by the film thickness. The enhancement of the crystallization with increasing film thickness produces the highly orientated film, but the films thicker than the critical thickness (≈500 nm) produce nonuniformity of the orientation of the films due to undesired heterogeneous nucleation. It is confirmed that the tetragonality of the PLT perovskite structure decreases with the increase of La content in the films. From the results of X-ray rocking curves, the films fabricated on c-plane sapphire substrates have better crystallographic alignment than those on the MgO (100) substrates due to a better lattice match between the film and the substrate. The a-axis orientation of the sol-gel processed PLT films on the MgO (100) substrate is determined only by the formation of the intrinsic tensile stress generated by the reducing the volume in the films during the crystallization.

Acknowledgements

This work has been supported by Korea Science and Engineering Foundation (Grant No.: 981-0803-019-2).

References

1. G. H. HAERTLING and C. E. LAND, *J. Amer. Ceram. Soc.* **54** (1971) 1.
2. T. KAWAGUCHI, H. ADACHI, K. SETSUNE, O. YAMAZAKI and K. WASA, *Appl. Opt.* **23** (1984) 2187.
3. H. HIGASHINO, T. KAWAGUCHI, H. ADACHI, T. MAKINO and O. YAMAZAKI, *Jpn. J. Appl. Phys.* **24** (24-2) (1985) 284.
4. G. H. HAERTLING, *Integrated Ferroelectrics* **3** (1993) 207.
5. H. ADACHI, T. KAWAGUCHI, K. KENTARO, K. OHJI and K. WASA, *Appl. Phys. Lett.* **42** (1983) 867.
6. F. WANG and G. H. HAERTLING, in Proceedings 8th IEEE Int. Symp. Appl. Ferroelectrics, Greenville, 1992, edited by M. Liu, A. Safari, A. Kingon and G. Haertling (IEEE) p. 596.
7. YOUNG MIN KANG, JA KANG KU and SUNGGI BAIK, *J. Appl. Phys.* **78** (1995) 2601.
8. G. YI, Z. WU and M. SAYER, *ibid.* **64** (1988) 2717.
9. C. K. BARINGAY and S. K. DEY, *Appl. Phys. Lett.* **61** (1992) 1278.
10. J. KOO, S.-U. KIM, D. S. YOON, K. NO and B.-S. BAE, *J. Mater. Res.* **12** (1997) 812.
11. G. TEOWEE, PhD thesis, University of Arizona, 1992, p. 21.
12. Y. LIU, W. REI, J. H. QIU, L. ZHANG and X. YAO, *Ferroelectrics* **152** (1994) 195.
13. M. OKUYAMA, T. USUKI and Y. HAMAKAWA, *Appl. Phys.* **21** (1980) 339.
14. H. ADACHI, T. MITSUYU, O. YAMAZAKI and K. WASA, *J. Appl. Phys.* **60** (1986) 736.
15. B.-S. BAE, W. J. LEE, K. NO, D. S. YOON and S.-U. KIM, in Proceedings of the Materials Research Society Symposium, San Francisco, CA, April 1995, Vol. 392, edited by B. W. Wessels, S. R. Marder and D. M. Walba (Materials Research Society, Pittsburgh, PA, 1995) p. 279.
16. R. TAKAYAMA, Y. TOMITA, K. IIJIMA and I. UEDA, *Ferroelectrics* **118** (1991) 325.
17. D. S. YOON, C. J. KIM, J. S. LEE, W. J. LEE and K. NO, *J. Mater. Res.* **9** (1994) 420.
18. Z. LI, C. M. FOSTER, D. GUE, H. ZHANG, G. R. BAI, P. M. BALDO and L. E. REHN, *Appl. Phys. Lett.* **65** (1994) 1106.
19. C. M. FOSTER, Z. LI, M. BUCKETT, D. MILLER, P. M. BALDO, L. E. REHN, G. R. BAI, D. GUO, H. YOU and K. L. MERKLE, *J. Appl. Phys.* **78** (1995) 2607.
20. H. FUNAKUBO, T. HIOKI, M. OTSU, K. SHINOZAKI and N. MIZUTANI, *Jpn. J. Appl. Phys. Pt. 1* **32**(9B) (1993) 4175.
21. H. M. CHOI and S. K. CHOI, *J. Vac. Sci. Technol. A* **13** (1995) 2832.
22. F. M. D'HEURLE and J. M. E. HARPER, *Thin Solid Films* **171** (1989) 81.
23. H. WINDISHMANN, *J. Vac. Sci. Technol. A* **9** (1991) 2431.
24. W. POMPE, X. GONG, Z. SUO and J. S. SPECK, *J. Appl. Phys.* **74** (1993) 6012.

Received 18 June 1998
and accepted 8 April 1999